

THE LATERAL DISTRIBUTION OF THE EFFECTIVE CONTACT POTENTIAL DIFFERENCE OVER THE GATE AREA OF MOS STRUCTURES

H. M. PRZEWLOCKI¹, A. KUDLA¹, D. BRZEZINSKA¹,
L. BOROWICZ¹, Z. SAWICKI¹, H. Z. MASSOUD²

¹Institute of Electron Technology, al. Lotników 32/46, 02-668 Warszawa, Poland

²Semiconductor Research Laboratory, Department of Electrical and Computer Engineering,
Duke University, Durham, NC 27708-0291, USA

Received December 11, 2003; published January 5, 2004

ABSTRACT

The lateral distribution of the effective contact potential difference (ECPD), often referred to as the work-function difference ϕ_{MS} , was determined experimentally for the first time over the gate area of a metal-oxide-semiconductor (MOS) structure. The photoelectric method for measuring ϕ_{MS} in MOS devices was modified to characterize the lateral distribution of ECPD. In square MOS gates, it is found that ϕ_{MS} values were highest in the center area of the gate, lower along the gate edges, and lowest at the gate corners. These results were confirmed by several independent photoelectric and electrical measurement methods. A model is proposed, in which the experimentally determined $\phi_{MS}(x,y)$ distributions, are attributed to mechanical stress distributions in MOS structures. Equations are derived allowing calculation of $\phi_{MS}(x,y)$ distributions for various structures. Results of these calculations remain in agreement with experimentally obtained distributions.

1. Introduction

Mechanical stress in a MOS structure is known to influence its electrical parameters [1, 2]. Among the parameters which are influenced by mechanical stress is the effective contact potential difference (ECPD), also called ϕ_{MS} . The influence of mechanical stress on the ϕ_{MS} value of a MOS structure was quantitatively estimated [3]. It is also known that mechanical stress is nonuniformly distributed under the gate of a MOS structure [2, 4, 5], and that it changes rapidly in the vicinity of the gate edges as shown in Fig. 1. It is therefore expected that ϕ_{MS} will have different values in the vicinity of gate edges and far away from them. This lateral distribution of ϕ_{MS} values has not been experimentally characterized to date because the electrical parameters determined by conventional techniques, including ϕ_{MS} , are averaged over the gate area. In this work, the lateral distribution of the ϕ_{MS} values over the gate area of MOS devices was measured for the first time. These results were obtained by modifying the photoelectric method for the determination of ϕ_{MS} [6]. The modifications of the photoelectric method are described elsewhere [7].

The photoelectric measurement results and their correlation with stress distributions in MOS structures were also supported by the electrical characteristics of these structures.

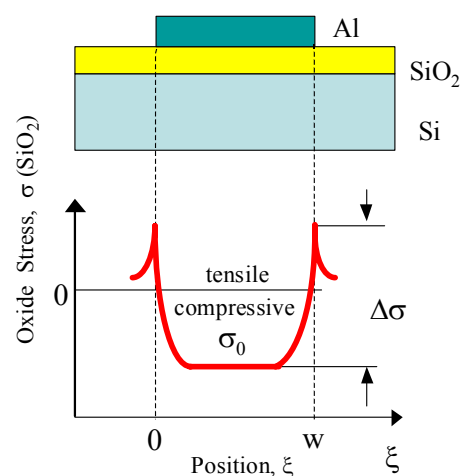


Fig. 1. A qualitative one-dimensional distribution of stress $\sigma(\xi)$ in the oxide layer under the aluminum gate. Here ξ designates a co-ordinate in any direction in the plane of the gate, and w is the width of the gate in the ξ direction.

A model of lateral distributions of ϕ_{MS} local values over the gate area has also been developed and is presented later. A range of measurement results fully supports the validity of the model.

2. Experimental

2.1. Measurement methods

The photoelectric ECPD measurement method [6] was modified by focusing the laser generated UV radiation into a beam of small diameter $D \approx 20 \mu\text{m}$, as illustrated in Fig. 2 and discussed elsewhere in more detail [7]. The gate area of a MOS capacitor is scanned with this beam of wavelength λ_{UV} and the photocurrent I vs gate voltage V_G characteristics are measured, allowing the determination of the zero-photocurrent voltage V_G^0 for each position of the UV light spot over gate area.

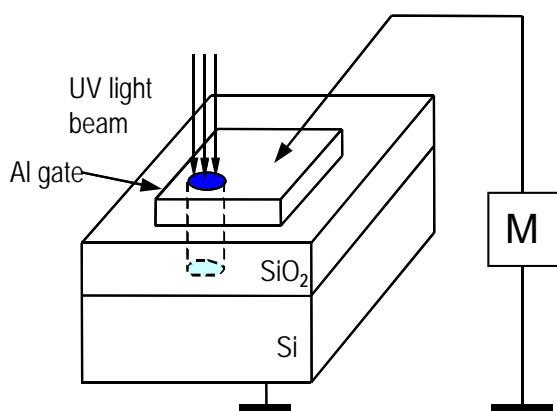


Fig. 2. Illustration of the principle of the modified photoelectric ϕ_{MS} determination method.

Analysis of these characteristics allows determination of the local ϕ_{MS} value in the illuminated region, as described in [6] and references therein. Hence, scanning the gate with the UV light beam allows determination of the lateral ϕ_{MS} distribution over the gate area. Results obtained using this method are verified using the purely electrical $C(V)$ measurements and using the photoelectric measurements made on entire MOS capacitors of different shapes and dimensions, as described later.

2.2. Measured structures

In this work, measurements were made on Al/SiO₂/n⁺-Si(100) and on Al/SiO₂/n-Si(100) capacitors of different geometries, processed as described in [3]. Although SiO₂ layers of current technological interest are thinner than 3 nm, larger values of oxide thickness: $X_{ox} = 20, 60$ and 160 nm were selected in order to optimize the sensitivity of the photoelectric methods [6]. Two aluminum gate thicknesses $X_{Al} = 35$ nm and 400 nm were used in this study. The

gates were square shaped with side $a = 0.1, 0.2, 0.5$ and 1 mm, with the perimeter-to-area ratio R of 4, 8, 20 and 40 respectively.

Besides, the photoelectric ϕ_{MS} measurements [6] were made on Al/SiO₂/n⁺-Si(111) capacitors with widely different R values, processed similarly as structures described above. The samples had an oxide thickness $X_{ox} = 60$ nm and aluminum gate thickness $X_{Al} = 35$ nm. The gates were either square-shaped or strip-shaped. The square-shaped gates were 1 x 1, 0.5 x 0.5, and 0.25 x 0.25 mm², with the perimeter-to-area ratio R of 4, 8, and 16, respectively. The strip-shaped gates were of two geometries. The first geometry was a square frame 1 mm on each side with the width of the aluminum lines being 0.02 mm, with a 0.1 x 0.1 mm² contact pad in one corner. The area of the aluminum gate was 0.0848 mm², the perimeter was 7.84 mm, and the perimeter-to-area ratio R of 92.5 mm⁻¹. The second geometry consisted of a set of 51 parallel aluminum lines 0.005 mm wide and 0.5 mm long. The separation between the strips was 0.005 mm. The strips were shorted at both ends with perpendicular aluminum lines of the same width. A 0.1 x 0.1 mm² contact pad was located in one corner of the gate. The area was 0.130 mm², the perimeter 51 mm, and the perimeter-to-area ratio R of 392.3 mm⁻¹.

2.3. Measurement results

Typical results of measurements made using the modified photoelectric method are shown in Fig. 3 in which the zero photocurrent voltage V_G^0 is shown in function of the co-ordinate ξ which is measured along the diagonal of the square gate or through the center of the gate and parallel to the gate edges.

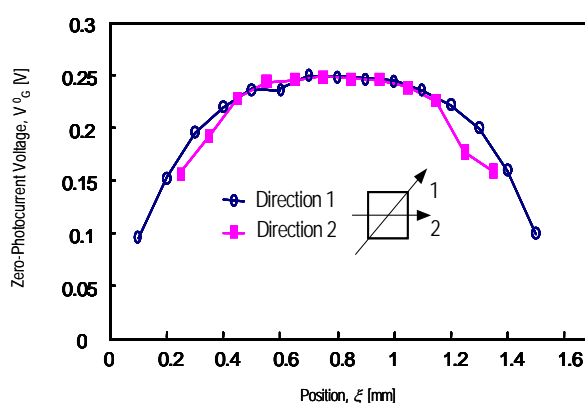


Fig. 3. Typical dependence of the zero-photocurrent voltage V_G^0 obtained at $\lambda_{UV} = 244$ nm on the position in Al/SiO₂/n⁺-Si structures with $X_{Al} = 400$ nm and $X_{ox} = 60$ nm. The direction is either (1) along the diagonal of the square gate, or (2) through the center of the square gate and parallel to its edges.

The V_G^0 voltage can be expressed as: $V_G^0(\lambda_{UV}) = \phi_{MS} + C(\lambda_{UV})$ [6], hence for a constant wavelength λ_{UV} used in the measurements, there is only a constant (and small) difference C between the

values of V_G^0 and ϕ_{MS} . In other words, the shape of the $V_G^0(\xi)$ dependence, shown in Fig. 3, is identical with the shape of the corresponding $\phi_{MS}(\xi)$ distribution. Hence, as shown in Fig. 3, the ϕ_{MS} values are highest in the middle of the gate, lower at gate edges, and lowest at gate corners. Such a distribution suggests that ϕ_{MS} values determined for the entire MOS structures, which are equal to $\phi_{MS}(x,y)$ distributions averaged over the gate area, should depend on the ratio R of the gate perimeter to gate area.

This expected dependence should be such, that ϕ_{MS} decreases with increasing R . This has been verified by making photoelectric ϕ_{MS} measurement [6], of MOS structures with widely different R values. Typical results of such measurements are shown in Fig. 4 fully supporting these expectations.

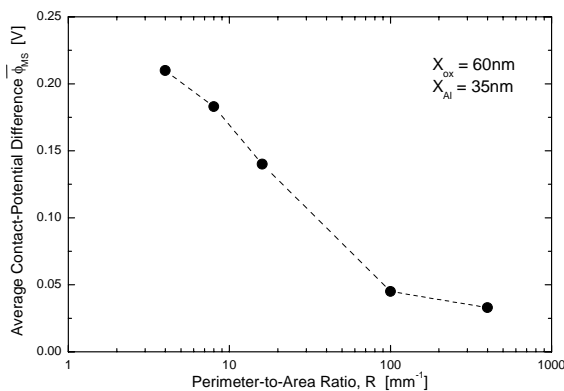


Fig. 4. Dependence of the effective contact potential difference ϕ_{MS} of Al/SiO₂/n⁺-Si MOS capacitors on the perimeter-to-area ratio R . Results are shown for square-gate MOS structures with $R = 4.8$ and 16 mm^{-1} , and for structures with gates in form of narrow aluminum lines, with $R \cong 100$ and 400 mm^{-1} respectively.

All the evidence presented above, of the nonuniform $\phi_{MS}(\xi)$ distributions is based on photoelectric measurements. Hence to exclude the possibility that the observed results are due to some unidentified optical effect, taking place when UV radiation illuminates the edges and corners of the gates, the results were confirmed by electrical measurements which do not involve the use of radiation. Taking into account that the ϕ_{MS} value directly influences the value of the flat-band voltage V_{FB} , capacitance-voltage $C(V_G)$ characteristics were taken for MOS structures with different R ratio, and V_{FB} values were determined from these characteristics. This way V_{FB} values were obtained for thousands of Al/SiO₂/n-Si capacitors, which were identically processed as the Al/SiO₂/n⁺-Si structures measured by photoelectric methods, as described above. Results of these measurements consistently show that flat-band voltage values decrease with increasing values of R . Typical results obtained for square gate capacitors, with $R = 4, 8, 20$ and 40 mm^{-1} are shown in Fig. 5, fully confirming the conclusions

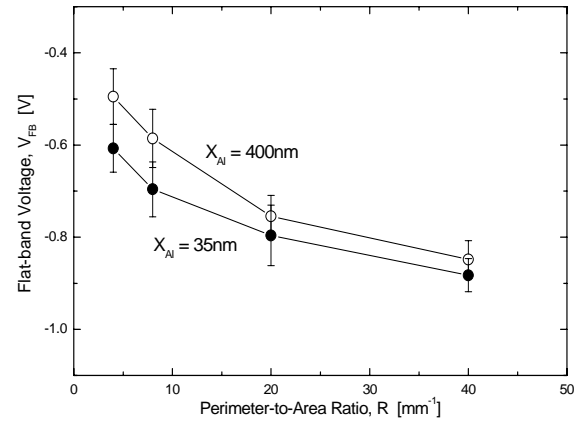


Fig. 5. Dependence of the average value and standard deviation of V_{FB} on the perimeter-to-area ratio R for square-gate Al/SiO₂/n-Si capacitors on the same silicon wafer. The $V_{FB}(R)$ dependencies are shown for capacitors with oxide thickness $X_{ox} = 60 \text{ nm}$ and different aluminum-gate thickness X_{Al} of 35 and 400 nm.

drawn from results obtained by photoelectric methods.

3. Model

Consider the one-dimensional stress distribution $\sigma(x)$ in the SiO₂-layer of a MOS capacitor, under the square shaped gate of side length a . The x -axis is assumed here to pass through the center of the gate and to be parallel to two of the gate edges, with the two other edges at $x = 0$ and $x = a$. Lets assume that the stress distribution $\sigma(x)$ can be modelled as:

$$\sigma(x) = \sigma_0 + \Delta\sigma(x) = \sigma_0 + \Delta\sigma \{ \exp(-x/\lambda_\sigma) + \exp[-(a-x)/\lambda_\sigma] \} \quad (1)$$

where σ_0 is the compressive stress in the central part of the gate, $\Delta\sigma = \Delta\sigma(0) = \Delta\sigma(a)$ is the maximum deviation of $\sigma(x)$ from the σ_0 value which occurs at gate edges (for $x = 0$ and $x = a$), and λ_σ is the characteristic length of the stress distribution. Assuming that the lateral ϕ_{MS} distribution is caused by lateral stress distributions, in such a way that $|\Delta\phi_{MS}(x)|$ is proportional to $\Delta\sigma(x)$, the one-dimensional $\phi_{MS}(x)$ distribution can be expressed as:

$$\phi_{MS}(x) = \phi_{MS,0} + \Delta\phi_{MS} \{ \exp(-x/\lambda_\sigma) + \exp[-(a-x)/\lambda_\sigma] \} \quad (2)$$

where $\phi_{MS,0}$ is the ϕ_{MS} value far away from gate edges, $\Delta\phi_{MS} = \Delta\phi_{MS}(0) = \Delta\phi_{MS}(a)$ is the deviation of $\phi_{MS}(x)$ from the $\phi_{MS,0}$ value which occurs at gate edges (for $x = 0$ and $x = a$), and as results from experiment $\Delta\phi_{MS}$ is negative.

The one-dimensional analysis, presented so far, can be applied to some of the MOS capacitors of practical interest, e.g. to structures with gates in form of long and narrow stripes, of width a and length l , used in our experiments.

The ratio R of the perimeter (P) to the area (A) of these gates is given by:

$$R = \frac{P}{A} = \frac{2(a+l)}{a \cdot l} \cong \frac{2}{a} \quad (3)$$

when length $l \gg a$.

The average value $\bar{\phi}_{MS}$ of one-dimensional distribution is defined as:

$$\bar{\phi}_{MS} \equiv \frac{1}{a} \int_0^a \phi_{MS}(x) dx. \quad (4)$$

Substituting Eq. (2) and Eq. (3) in Eq. (4) leads to:

$$\bar{\phi}_{MS} = \phi_{MS,0} + \Delta\phi_{MS} \cdot \lambda_{\sigma} \cdot R \left[1 - \exp\left(-\frac{2}{\lambda_{\sigma} \cdot R}\right) \right]. \quad (5)$$

However, in most of the cases, the problem considered is not of a one-dimensional nature. For instance, for structures with square gates, of side length a , lying in the x,y plane, the $\Delta\sigma(x)$ and $\Delta\phi_{MS}(x)$ distributions are equally important as $\Delta\sigma(y)$ and $\Delta\phi_{MS}(y)$. Assuming that the properties of the MOS system are isotropic in the x,y plane, these distributions can be expressed by Eqs. (1) and (2), and analogous equations with the x variable replaced by y . Assuming further that the principle of superposition can be applied to stress and ECPD distributions in the x,y plane, one obtains:

$$\Delta\phi_{MS}(x,y) = \Delta\phi_{MS}(x) + \Delta\phi_{MS}(y), \quad (6)$$

and:

$$\phi_{MS}(x,y) = \phi_{MS,0} + \Delta\phi_{MS}(x,y). \quad (7)$$

Equations (7) and (6), together with expressions for $\Delta\phi_{MS}(x)$ and $\Delta\phi_{MS}(y)$, analogous to Eq. (2), determine the $\phi_{MS}(x,y)$ distribution in the x,y plane of the gate area. Examples of $\phi_{MS}(x,y)$ distributions, calculated using the above equations, for structures with square gates of different side lengths a are shown in Fig. 6.

For such structures the average ϕ_{MS} value, designated $\bar{\phi}_{MS}$, is given by:

$$\bar{\phi}_{MS} = \frac{1}{a^2} \int_0^a \int_0^a \phi_{MS}(x,y) dx dy. \quad (8)$$

The integration of Eq. (7) yields:

$$\bar{\phi}_{MS} = \phi_{MS,0} + 4 \frac{\Delta\phi_{MS} \cdot \lambda_{\sigma}}{a} \left[1 - \exp\left(-\frac{a}{\lambda_{\sigma}}\right) \right] \quad (9)$$

showing that $\bar{\phi}_{MS}$ is a function of a/λ_{σ} , as clearly seen in Fig. 6. Equation (9) can be transformed to explicitly give the dependence of ϕ_{MS} on the previously introduced perimeter to area ratio, $R = 4/a$ for square gates.

$$\bar{\phi}_{MS} = \phi_{MS,0} + \Delta\phi_{MS} \cdot \lambda_{\sigma} \cdot R \left[1 - \exp\left(-\frac{4}{\lambda_{\sigma} \cdot R}\right) \right]. \quad (10)$$

The $\bar{\phi}_{MS}(R)$ dependence is reflected in the dependence of the flat-band voltage \bar{V}_{FB} (measured on the entire MOS structure) on R . Assuming that the effective charge of the MOS system does not

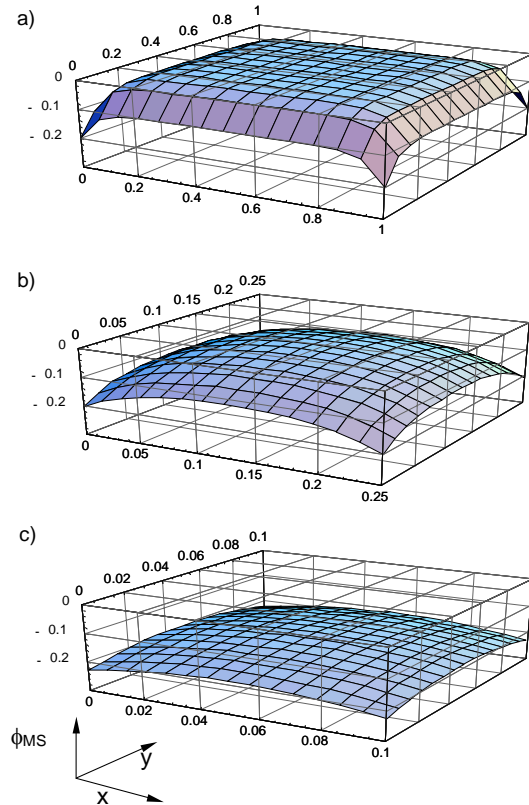


Fig. 6. The $\phi_{MS}(x,y)$ distribution calculated using the model, for square gate Al-SiO₂-Si capacitors of different side length a : a) $a = 1$ mm, b) $a = 0.25$ mm, c) $a = 0.1$ mm, and using $\phi_{MS,0} = 0$ V, $\Delta\phi_{MS} = -0.1$ V, $\lambda_{\sigma} = 0.05$ mm in the expressions for $\Delta\phi_{MS}(x)$ and $\Delta\phi_{MS}(y)$.

significantly depend on R , the $\bar{V}_{FB}(R)$ dependence for square gate structures is:

$$\bar{V}_{FB} = V_{FB,0} + \Delta V_{FB} \cdot \lambda_{\sigma} \cdot R \left[1 - \exp\left(-\frac{4}{\lambda_{\sigma} \cdot R}\right) \right] \quad (11)$$

where $V_{FB,0}$ is the local $V_{FB}(x,y)$ value far away from the gate edges, and $|\Delta V_{FB}|$ is maximum deviation of $V_{FB}(x,y)$ from the $V_{FB,0}$ value (ΔV_{FB} is negative). Equations (5), (10), (11) are the equations of the model which can be used to determine $\bar{\phi}_{MS}(R)$ and $\bar{V}_{FB}(R)$ dependencies in MOS structures, as verified below.

4. Verification

To verify the model, experimental results were fit with the model equations. The best fit of model equations to the measurement results yields the model parameters for a given set of experiments, i.e. the values of $\phi_{MS,0}$, $\Delta\phi_{MS}$ and λ_{σ} or $V_{FB,0}$, ΔV_{FB} and λ_{σ} .

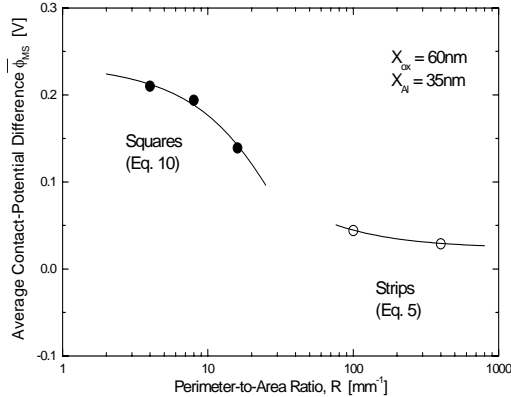


Fig. 7. Experimental results and model predictions of the dependence of $\bar{\phi}_{MS}$ on the perimeter-to-area ratios R . For square-gate MOS structures with low values of R , the experimental data is plotted using solid circles \bullet and the model is given by Eq. (10), using $\phi_{MS,0} = 0.236$ V, $\Delta\phi_{MS} = -0.106$ V, and $\lambda_{\sigma} = 0.056$ mm. For structures with strip-shaped gates with large ratios R , the experimental data is plotted using open circles \circ and the model is given by Eq. (5), using $\phi_{MS,0} = 0.236$ V, $\Delta\phi_{MS} = -0.106$ V, and $\lambda_{\sigma} = 0.096$ mm.

As an example, model Eqs. (5) and (10) were fit to the ϕ_{MS} measurement results obtained for MOS structures with different gate shapes, made on the same silicon wafer, as shown by the lines in Fig. 7. It should be noted that for both the square and strip-type structures the fit is obtained for the same $\phi_{MS,0}$ and $\Delta\phi_{MS}$ values, which strongly supports the validity of the model. The (effective) λ_{σ} value is different for square and strip structures, since for strip structures λ_{σ} is comparable to the width a of the aluminum lines and the influences of both line edges overlap.

The model was further verified by fitting Eq. (11) to the V_{FB} measurement results. As an example, Eq. (11) is fit to the measurement results, as shown by the lines in Fig. 8. It should be noted that the best fit gives higher values of both $V_{FB,0}$ and $|\Delta V_{FB}|$ for structures with thicker gates. This is the result that was expected since thicker aluminum layers cause higher compressive stresses σ_0 in the SiO_2 layer and larger $\Delta\sigma$ deviations at gate edges, supporting the assertion that the lateral distributions of ϕ_{MS} and V_{FB} values are caused by lateral distributions of stress $\sigma(\text{SiO}_2)$, in the plane of the gate. Further support for this assertion was gained from an experiment based on the following reasoning. Any change in the stress distribution under the MOS system gate, should be reflected in changes of ϕ_{MS} and V_{FB} distributions.

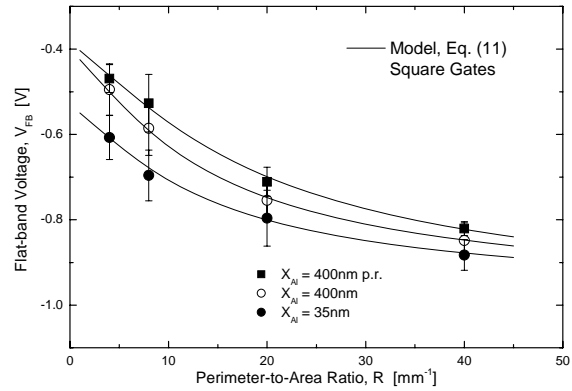


Fig. 8. Experimental results and model predictions of the dependence of the flat-band voltage V_{FB} on the perimeter-to-area ratio R for square-shaped MOS gates. Structures with an aluminum gate thickness of $X_{Al} = 35$ nm, $X_{ox} = 60$ nm are plotted using solid circles \bullet , these of structures with an aluminum gate thickness of $X_{Al} = 400$ nm, $X_{ox} = 60$ nm are plotted using open circles \circ , those of structures with $X_{Al} = 400$ nm – thick aluminum gate surrounded by protective aluminum rings (p.r.) are plotted using solid squares \blacksquare . The model is given by Eq. (11) and the best fit was obtained using for MOS structures:

- \bullet $V_{FB,0} = -0.530$ V, $\Delta V_{FB} = -0.115$ V, $\lambda_{\sigma} = 0.17$ mm,
- \circ $V_{FB,0} = -0.400$ V, $\Delta V_{FB} = -0.148$ V, $\lambda_{\sigma} = 0.17$ mm,
- \blacksquare $V_{FB,0} = -0.384$ V, $\Delta V_{FB} = -0.161$ V, $\lambda_{\sigma} = 0.12$ mm.

A change of stress distribution can be introduced if a gate of another MOS structure is placed close enough to the gate of investigated structure. Hence, a comparison was made between the $V_{FB}(R)$ characteristics of square gate capacitors, which were not surrounded by other capacitors in their immediate vicinity, with the characteristics of identical capacitors surrounded by protective aluminum rings of the same thickness $X_{Al} = 400$ nm, at a distance of 10 μm . Similarly as in the case of capacitors with different aluminum gate thickness (see Fig. 8), a considerable shift is observed between the $V_{FB}(R)$ characteristics of structures with and without the protective aluminum rings.

5. Conclusions

The lateral distribution of local ECPD values over the gate area of a MOS structure was studied for the first time. Photoelectric and electrical measurement methods were used in this investigation. It was found that ϕ_{MS} has a characteristic distribution over the gate area, with local ϕ_{MS} values being highest in the middle of the gate, lower at gate edges, and lowest at gate corners. To study these ECPD distributions, the photoelectric ϕ_{MS} measurement method was modified, allowing determination of local ECPD values over dimensions that are small in comparison with the gate dimensions of the MOS structure. The lateral distributions of ECPD are attributed to lateral distributions of mechanical stress under the gate of a MOS structure. A simple model is proposed of the

distribution of local ϕ_{MS} values over the gate area. The $\phi_{MS}(x,y)$ distributions calculated using this model remain in agreement with the ones determined by the photoelectric method. The validity of the model is further verified by electrical measurements of the flat-band voltage V_{FB} values of a range of Al-SiO₂-Si capacitors, differing in the ratio R , of the gate perimeter to gate area.

REFERENCES

1. C. H. BJORKMAN, J. T. FITCH, G. LUCOVSKY, *Appl. Phys. Lett.*, 1990, **56**, 1983–1985.
2. S. M. HU. *J. Appl. Phys.*, 1991, **70**, R53–R80.
3. H. M. PRZEWOŁOCKI, H. Z. MASSOUD, *J. Appl. Phys.*, 2002, **92**, 2198–2201.
4. I. DE WOLF, H. E. MAES, S. K. JONES. *J. Appl. Phys.*, 1996, **79**, 7148–7156.
5. K. F. DOMBROWSKI, I. DE WOLF, B. DIETRICH, *Appl. Phys. Lett.*, 1999, **75**, 2450–2451.
6. H. M. PRZEWOŁOCKI, *Solid St. Electron.*, 2001, **45**, 1241–1250.
7. A. KUDŁA, H. M. PRZEWOŁOCKI, L. BOROWICZ, D. BRZEZIŃSKA, W. RZODKIEWICZ, *Photoelectrical Measurements of the Local Value of the Contact Potential Difference in the Metal-Insulator-Semiconductor (MIS) Structures*. Symp. on Optical and X-Ray Metrology for Advanced Device Materials Characterization. E-MRS 2003 Spring Meet. Strasbourg, France, 10–13 June 2003. To be published in *Thin Solid Films*.